Journal Pre-proof

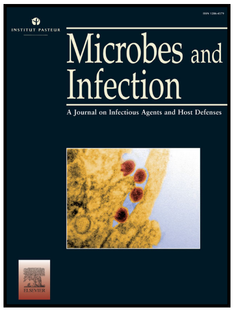

Extracellular vesicles secreted by *Echinococcus multilocularis:* Important players in angiogenesis promotion

Congshan Liu, Jianping Cao, Haobing Zhang, Mark C. Field, Jianhai Yin

PII: S1286-4579(23)00050-3

DOI: https://doi.org/10.1016/j.micinf.2023.105147

Reference: MICINF 105147

To appear in: *Microbes and Infection*

Received Date: 25 October 2022

Revised Date: 26 April 2023

Accepted Date: 28 April 2023

Please cite this article as: C. Liu, J. Cao, H. Zhang, M.C. Field, J. Yin, Extracellular vesicles secreted by *Echinococcus multilocularis:* Important players in angiogenesis promotion, *Microbes and Infection*, https://doi.org/10.1016/j.micinf.2023.105147.

Extracellular vesicles secreted by *Echinococcus multilocularis:* Important players in angiogenesis promotion

Congshan Liu [a], Jianping Cao [a], Haobing Zhang [a], Mark C. Field [b,c], Jianhai Yin [a, *]

[a] *National Institute of Parasitic Diseases, Chinese Center for Disease Control and Prevention (Chinese Center for Tropical Diseases Research); NHC Key Laboratory of Parasite and Vector Biology; WHO Collaborating Center for Tropical Diseases; National Center for International Research on Tropical Diseases, Shanghai 200025, China*
[b] *School of Life Sciences, University of Dundee, Dundee, DD1 5EH, UK*
[c] *Institute of Parasitology, Czech Academy of Sciences, České Budějovice, Czech Republic*

Corresponding author:

E-mail address: yinjh@nipd.chinacdc.cn (J Yin)

Abstract

The involvement of *Echinococcus multilocularis,* and other parasitic helminths, in regulating host physiology is well recognized, but molecular mechanisms remain unclear. Extracellular vesicles (EVs) released by helminths play important roles in regulating parasite-host interactions by transferring materials to the host. Analysis of protein cargo of EVs from *E. multilocularis* protoscoleces in the present study revealed a unique composition exclusively associated with vesicle biogenesis. Common proteins in various *Echinococcus* species were identified, including the classical EVs markers tetraspanins, TSG101 and Alix. Further, unique tegumental antigens were identified which could be exploited as *Echinococcus* EV markers. Parasite- and host-derived proteins within these EVs are predicted to support important roles in parasite-parasite and parasite-host communication. In addition, the enriched host-derived protein payloads identified in parasite EVs in the present study suggested that they can be involved in focal adhesion and potentially promote angiogenesis. Further, increased angiogenesis was observed in livers of mice infected with *E. multilocularis* and the expression of several angiogenesis-regulated molecules, including VEGF, MMP9, MCP-1, SDF-1 and serpin E1 were increased. Significantly, EVs released by the *E. multilocularis* protoscolex promoted proliferation and tube formation by human umbilical vein endothelial cells (HUVECs) *in vitro*. Taken together, we present the first evidence that tapeworm-secreted EVs may promote angiogenesis in *Echinococcus*-infections, identifying central mechanisms of *Echinococcus*-host interactions.

KEYWORDS

Echinococcus multilocularis, protoscoleces, extracellular vesicle, exosome, proteomics, angiogenesis

Abbreviations: CE, cystic echinococcosis; AE, alveolar echinococcosis; HF, hydatid fluid; PSCs, protoscoleces; EVs, extracellular vesicles; PBMCs, peripheral blood mononuclear cells; HUVECs, human umbilical vein endothelial cells; HBSS, Hank's balanced salt solution; PBS, phosphate buffered saline; FBS, fetal bovine serum; BSA, bovine serum albumin; VEGF, vascular endothelial growth factor; DAPI, 4', 6-diamidyno-2-fenyloindol; TEM, transmission electron microscopy; Exo, exosome; MVs, microvesicles; ILVs, intraluminal vesicles; HSPs, heat shock proteins; HSP70, heat shock protein 70; SDS-PAGE, SDS-polyacrylamide gel electrophoresis; TSG101, tumor susceptibility 101; MMP9, matrix metallopeptidase 9; MCP-1, monocyte chemoattractant protein-1; SDF-1, stromal cell derived factor 1; Serpin E1, plasminogen activator inhibitor-1; ESCRT, endosomal sorting complexes required for transport; HRS, hepatocyte growth factor-regulated tyrosine kinase substrate; STAM1, signal transducing adaptor molecule 1; SRA, serum resistance-associated.

Introduction

Echinococcosis is one of the most severe zoonoses and is caused by the larval form (metacestode) of *Echinococcus* genus cestodes. Infections cause serious social and economic burdens associated with the cost of treatment and livestock production losses [1-3]. There are at least eight *Echinococcus* species. Among them, *E. granulosus* and *E. multilocularis* are the major pathogens responsible for cystic echinococcosis (CE, which is globally distributed) and alveolar echinococcosis (AE, which is restricted to the Northern hemisphere), respectively [1, 2]. After ingesting parasite eggs, oncospheres hatch in the intestine and subsequently develop into metacestodes, mainly located in liver. Mature metacestodes contain hydatid fluid (HF) and can be filled with bundles of protoscoleces (PSCs) [4]. *E. multilocularis,* which grows into a tumour-like structure in the host liver, can lead to death [1, 4], partially attributed to the interplay between parasite and host, but mechanistic issues remain unaddressed. Recent evidence indicates that these parasites secrete extracellular vesicles (EVs) to facilitate modifying the local environment [5-17].

Both prokaryote and eukaryote cells release EVs, small membrane-bound secreted vesicles that can be subdivided into microvesicles (ectosomes, or microparticles, 50 nm to 1 μm in diameter), which pinch off from the surface of the plasma membrane via outward budding, and exosomes (40 to 160 nm in diameter), which are derived from endosomes [5-7]. EVs can contain nucleic acids, lipids, metabolites and cytosolic and cell-surface proteins, depending on their cellular origin, and are considered as a means to remove excess and/or unnecessary components from cells to maintain cellular homeostasis, or to participate in intercellular communication, and can also contribute towards emergence of pathology [5-7]. Many parasites employ multipurpose EVs in communication for persistence, development, transfer of virulence factors, adherence to host tissues, evasion of immune responses and modulation of the host [8, 9]. For example, the composition of EVs released by *Leishmania donovani* altered with temperature and pH changes [10], and malaria parasite DNA-harbouring EVs could activate STING-mediated DNA-sensing pathways and initiate a type I interferon responses [11]. *E. granulosus* exosome-like vesicles could be internalized by murine dendritic cells and induce their maturation with increased CD86 and down-regulation of MHC class II [12]. Moreover, some parasites such as *Leishmania spp. Plasmodium spp. and T. cruzi release EVs that* induce pro-inflammatory cytokine responses to promote pathogenesis (*etc*.), while *T. gondii*, *T. muris*, *H. polygyrus*, *N. brasiliensis* and *E. caproni* EVs inhibit or delay pathogenesis [9]. In addition, EVs may have potential for vaccine, therapeutic or diagnostic purposes [8, 9].

Echinococcus metacestodes mainly reside in liver of the mammalian host and interact with a microenvironment composed of immune cells, fibroblasts, endothelia and other cell types [4, 13]. Metacestodes orchestrate a series of outcomes that balance infection burden and host survival [14], and metacestode surface molecules and excretory/secretory metabolic products function as key players in these processes [13, 15]. Although *Echinococcus* species lack digestive and excretory systems, they possess endocytic and exocytic intracellular pathways that regulate metabolite uptake and release [12]. In addition, EVs released from *Echinococcus* spp. could participate in pathogen-host interactions. For example, parasite EVs could be internalized by dendritic cells, peripheral blood mononuclear cells (PBMCs), macrophages and T lymphocytes to modulate immune responses [12, 16-19]. Furthermore, among the proteins identified in parasite-derived EVs, some likely act as immunomodulators [20-22], while ncRNA (miRNAs, cirRNAs etcetera) [23, 24] have multiple functions, including as virulence factors [25], and inhibiting UBE2N, a ubiquitin-ligase with important roles in inflammatory and immune signal transduction in hepatocytes during *E. multilocularis* infection [26].

Neither the protein composition of *E. multilocularis* PSCs EVs or their impact on human umbilical vein endothelial cells (HUVECs) is known. Pro-angiogenic factors VEGF (vascular endothelial growth factor) and endothelial cells marker CD31 are highly expressed in host tissues proximal to *E. granulosus* lesions and accompanied by angiogenesis , described both by us and others [27-30]. Here we systematically characterized the protein cargo of EVs released by *E. multilocularis* PSCs and investigate their effects on HUVECs to explore their potential pro-angiogenic activity.

1. Methods

1.1 Ethics statement

Experiments involving mice were in strict accordance with Guidelines for the Care and Use of Laboratory Animals produced by the Shanghai Veterinary Research Institute. This study was approved by the Ethics Committee of the National Institute of Parasitic Diseases, Chinese Center for Disease Control and Prevention (license number IPD-2017-20).

1.2 E. multilocularis *maintenance and culture*

E. multilocularis was maintained in BALB/c mice (Shanghai SLAC Laboratory Animal Co., Ltd, Shanghai, China). In brief, mice were challenged with 2000 *E. multilocularis* PSCs via abdominal intraperitoneal transplantation passage for six months [31]. Parasite material was isolated from the peritoneal cavity of infected animals and homogenised in Hank's balanced salt solution (HBSS, Thermo Fisher Scientific, Carlsbad, CA, USA). After passing parasite homogenate through a 60-mesh sieve, *E. multilocularis* PSCs were collected and exhaustively washed with phosphate-buffered saline (PBS, Thermo Fisher Scientific, Carlsbad, CA, USA). The viability of these PSCs was determined by methylene blue exclusion and PSCs with viability >95% were used in subsequent experiments. About 10,000 PSCs/ml were cultured in 2 ml DMEM culture medium (Thermo Fisher Scientific, Carlsbad, CA, USA), supplemented with 10% FBS (v/v) (Thermo Fisher Scientific, Carlsbad, CA, USA) and antibiotics (100 U/ml penicillin G and 100 μg/ml streptomycin) (Thermo Fisher Scientific, Carlsbad, CA, USA) at 37 °C in 5% CO_2 for 24 to 48 hrs. Twenty-four hrs before collecting, the medium was replaced with FBS-free DMEM. PSCs were collected and homogenised in lysis buffer (Thermo Fisher Scientific, Carlsbad, CA, USA, cat# 78430) supplemented with protease and phosphatase inhibitors (Thermo Fisher Scientific, Carlsbad, CA, USA). After centrifuging at 8000 x *g* for 15 mins, supernatants were transferred to a new tube without disturbing the pellet as the whole PSCs lysate.

1.3 Extracellular vesicle isolation

A total exosome isolation kit (Thermo Fisher Scientific, Carlsbad, USA) was used for EVs isolation according to the manufacturer's instructions. In brief, 18 ml FBS-free PSC culture medium from three batches of collections was filtered through 0.22 µm PVDF filtered syringes (Millipore, Massachusetts, USA), and 0.5 volumes of total exosome isolation reagent added to collected FBS-free DMEM medium. The mixture was vortexed and incubated at 4°C overnight, then centrifuged at 10, 000 x *g* for 1 hr at 4°C. To remove contaminants, the resulting pellet was washed with PBS, centrifuged (10, 000 x *g* for 1 hr at 4 °C) and resuspended in PBS. The protein concentration of PSC lysis supernatants and EVs (solubilised in 2x lysis buffer) was determined with a BCA protein assay kit (Beyotime Biotechnology, Shanghai, China); 10 µg of EV suspension was used in all experiments unless specified. EV suspensions were stored at -80°C until analysis.

1.4 Western blotting

Samples were treated with lysis buffer (Thermo Fisher Scientific, Carlsbad, CA, USA) at 4°C and centrifuged at 8000 × *g* for 15 mins. Protein concentration was estimated by BCA protein assay kit (Beyotime Biotechnology, Shanghai, China). 10 µl samples containing 10 µg *E. multilocularis* PSCs EVs or *E. multilocularis* PSCs culture medium were separated by 10% SDS-PAGE (Thermo Fisher Scientific, Carlsbad, CA, USA) and transferred to a 0.45 µm PVDF membrane (Millipore, Burlington, MA, USA). The membrane was blocked for 1 hr with 5% non-fat milk (w/v, in 0.1% Tween® 20/PBS) (non-fat milk: Solarbio, Beijing, China; Tween® 20: Sigma-Aldrich, Saint Louis, USA) and incubated with anti-CD63 (Abcam, Cambridge, UK, cat# ab134045) and anti-TSG101 (Abcam, Cambridge, UK, cat# ab83) as primary antibodies (1/2000 in 5% non-fat milk) at 4°C overnight to detect cross-reactivity with *E. multilocularis* proteins of approximately 50 and 47 kDa respectively, then incubated with a 1/5000 dilution of goat anti-rabbit IgG antibody (Abcam, Cambridge, UK, cat# ab6721) conjugated with HRP as a secondary antibody at room temperature for 1 hr and washed again. ECL Western Blot substrate (Thermo Fisher Scientific, Carlsbad, CA, USA) was used to visualize bound antibody.

1.5 Transmission electron microscopy

Extracellular vesicles were fixed in 2.5% glutaraldehyde (w/v) (Sigma-Aldrich, Saint Louis, USA) and placed onto 300-mesh copper grids with carbon-coated formvar film and incubated for 5 mins. Excess liquid was removed and the grid negatively stained with saturated uranylacetate (Sinopharm Chemical Reagent Co., Ltd., Shanghai, China) for 1 min, followed by again removing excess liquid. EVs were examined at 100 kV in a FEI Tecnai G2 Spirit transmission electron microscope (FEI Company, Oregon, USA). EV sizes were calculated from eight random fields (Table S01, Figure S1) using ImageJ software [32], applying a stringent method for enumerating EVs in which only objects that presented a well-defined near-to-circular or tubular morphology were considered.

PSCs were fixed with 2.5% glutaraldehyde (w/v) (Sigma-Aldrich, Saint Louis, USA) at 4 °C for 24 hrs, washed three times with PBS (pH7.4) and post-fixed in 2% Osmium tetroxide at 4 °C for 2 hrs. After dehydration in a graded series of ethanol (Sinopharm Chemical Reagent Co., Ltd., Shanghai, China) and embedding with Pon812 embedding kit (SPI, West Chester, PA, USA), 70 nm ultrathin sections were cut on a Leica EM UC7 Ultramicrotome (Illinois, USA), placed on copper grids, and stained with uranyl acetate and lead citrate (Sinopharm Chemical Reagent Co., Ltd., Shanghai, China). Grids were examined with a FEI Tecnai G2 Spirit TEM instrument.

1.6 Proteomic analysis

30 µg PSC lysate, PSC culture medium and purified PSC EVs were sent to the Majorbio proteomic service (Shanghai, China) for mass spectrometry analysis. Briefly, samples were treated with 10 mM tris-2-carboxyethyl-phosphine (Thermo Fisher Scientific, Carlsbad, USA) in 100 mM triethylammonium bicarbonate buffer (Sigma-Aldrich, Saint Louis, USA) at 37°C for 60 min, followed by alkylation with 40 mM iodoacetamide (Sigma-Aldrich, Saint Louis, USA) for 40 min at room temperature, in darkness. After adding six volumes of cold acetone (Sinopharm Chemical Reagent Co., Ltd., Shanghai, China) at -20°C for 4 hrs, pellets were digested with trypsin (Promega, Madison, USA) and analysed with an EASY-nLC 1200 system (Thermo Fisher Scientific, West Palm Beach, FL, USA) coupled to a Q-Exactive HF-X mass spectrometer (Thermo Fisher Scientific, Carlsbad, USA) to separate and identify peptides.

Analysis of spectra was carried out using Xcalibur 4.0. After searching in SwissProt/UniProt *E. multilocularis* (Taxon ID: 6211), *M. musculus* (Taxon ID: 10090) and *Bos taurus* (Taxon ID: 9913) databases with PEAKS Studio 8.5, proteins selected by unique peptide > 1, 10logP >= 20 were analysed further. All searches were conducted with the following parameters: trypsin cleavage at both termini and two missed cleavage sites allowed; 10 ppm for precursor mass tolerance; 0.05 Da for fragment mass tolerance; cysteine carbamidomethylation as static modification, methionine oxidation and acetylation as dynamic modifications. *In silico* analyses to establish Gene Ontology (GO) and Kyoto Encyclopedia of Genes and Genomes (KEGG) classification was performed using the UniProt database (http://www.uniprot.org/), DAVID bioinformatics resources (https://david.ncifcrf.gov/), KEGG (https://www.kegg.jp/) and KOBAS (http://kobas.cbi.pku.edu.cn/). Proteins identified as uncharacterized, hypothetical, conserved or expressed protein were classified based on the presence of conserved domains using CDD (https://www.ncbi.nlm.nih.gov/cdd/).

1.7 Comparative analysis of extracellular vesicle protein cargo across several cestode species

There are seven [12, 16-18, 21, 22, 33] and four [34-37] publications describing EVs protein datasets of *Echinococcus* spp. and other cestodes, respectively. Due to differences in annotation between these studies, conserved domains identified by CDD (https://www.ncbi.nlm.nih.gov/cdd/) were used for comparative analysis across several cestode species. UpSetR package was used to determine the extent of common and/or unique domains [38].

1.8 Mouse angiogenesis array analysis
Liver tissue (n=3) surrounding *E. multilocularis*-infected lesions and from uninfected mice were homogenised in PBS with protease inhibitors (Sigma-Aldrich, Saint Louis, USA, cat#4693124001). After homogenisation, 1% Triton X-100 (v/v) was added and samples were frozen at -80°C. After thawing, tissue lysates were centrifuged at 10,000 x g for 10 mins, and the supernatant collected and protein estimated using BCA protein assay kit. A total of 300 µg tissue lysates from each group was used for angiogenesis array analysis using the mouse angiogenesis array (R&D systems, Minneapolis, USA, cat# ARY015), following the manufacturer's instructions. Membranes were scanned using a fluorescence chemiluminescence imaging system (Chemi Scop2 6300, Clinx Science Instruments Co., Ltd., Shanghai, China), and quantified using NIH ImageJ [32].

1.9 Immunofluorescence and immunohistochemistry
Liver tissues (n=2) from *E. multilocularis*-uninfected and -infected mice were fixed with 4% paraformaldehyde (w/v) and processed for immunohistochemistry (Wuhan Servicebio Technology Co. Ltd., Wuhan, China). Unless specifically noted, all reagents used are products of Wuhan Servicebio Technology Company. After dehydration with gradient alcohol (5% alcohol for 4 hrs, 85% alcohol for 2 hrs, 90% alcohol for 2 hrs, 95% alcohol for 1 hr, anhydrous ethanol II for 30 mins, anhydrous ethanol II for 30 mins) (Sinopharm Chemical Reagent Co., Ltd., Shanghai, China), tissue samples were cleared and embedded in paraffin, dissected to 4 µm thickness and affixed to slides. Before staining, slides were processed by deparafinization, rehydration, antigen retrieval and blocking of endogenous peroxidase activity.

For immunofluorescence, slides were blocked in 3% bovine serum albumin (BSA, w/v in 0.3% Triton™ X-100/PBS) for 30 mins, incubated with anti-CD63 (1/500 in 1% BSA) primary antibodies at 4°C overnight followed by incubation with 1/300 dilution of CY3-conjugated goat anti-rabbit IgG at room temperature for 1 hr. After washing with PBS (pH7.4), slides were stained with DAPI, dehydrated, mounted and visualized with a fluorescence microscope (Nikon, Tokyo, Japan).

For immunohistochemistry, slides were blocked in 3% BSA for 30 mins, and incubated with anti-CD31 (1/100) or anti-VEGF (1/200) as primary antibodies at 4 °C overnight, incubated with 1/200 dilution of HRP-conjugated goat anti-rabbit IgG or rabbit anti-goat IgG antibody at room temperature for 1 hr. After washing with PBS pH7.4, slides were stained with DAB (brown) and Harris hematoxylin stain solution (blue), and finally dehydrated, mounted and visualized under an inverted microscope (Nikon, Tokyo, Japan).

Vascular endothelial cells that stained positively for CD31 were quantified to record micro-vessel density (MVD), assessed by counting all stained vessels at 400x magnification in six random fields. The mean number of vessels was defined as the MVD. Positive staining for VEGF expression, indicating angiogenesis, was assessed at 400-times magnification in six random fields. Standardized analysis of pixel density with ImageJ [32] was used to quantitate CD31/VEGF-positive area(s).

1.10 HUVEC culture, cell proliferation and tube formation assays
HUVECs (Sciencell Research Laboratories, Carlsbad, CA, USA) were cultured and

maintained according to the supplier's instructions. All of the following assays were conducted using low passage cells (3-5 passages). In brief, cryopreserved primary cells were thawed into an equilibrated fibronectin-coated T-75 flask. Once the culture reached 90% confluence, cells were harvested and seeded in 96-well microtiter plates at 1×10^5 cells/ml in endothelial cell medium and allowed to attach for 24 hrs at 37 °C under 5% CO_2 before stimulating. After adding stimulus (10 µg total protein), plates were incubated for 48 hrs and cell viability determined with a cell counting kit-8 (Dojindo Laboratories, Kamimashiki-gun, Japan).

The effect of *E. multilocularis* material on HUVEC differentiation was examined by tube formation in Matrigel culture (BD Biosciences, San Diego, USA). HUVECs at > 90% confluence were harvested and diluted to 3×10^5 cells/ml. 100 µL of HUVEC suspension was mixed with 100 µL stimulus (10 µg total protein) diluted with DMEM and placed in 96-well plates at 37°C, 5% CO_2. Capillary networks were visualized under an inverted microscope (Nikon, Tokyo, Japan) and branch lengths in four random fields per well quantified using the angiogenesis module of ImageJ [32]. The experiments were repeated twice with triple replicates for each experiment.

1.11 Statistical analysis

SPSS software (IBM spss statistics professional authorized user, version 26.0) was used for statistical analysis. Differences between or among groups were analyzed using Student's t test/one way ANOVA and considered significant if the *P* value was < 0.05.

2. Results

2.1 E. multilocularis *protoscolex produces exosome-like vesicles*

Many EVs contain cellular components such as nucleic acids and proteins, which influence various biological pathways in recipient cells and tissues. EV pools with a typical cup-shaped morphology, confirmed by TEM analysis, were isolated from cultured *E. multilocularis* PSCs (Fig. 1A), with a diameter varying between 40 and 110 nm, mean 60.6 ± 15.8 nm (Fig. 1B). Immunoblotting indicated that these EVs contain known exosomal markers, including CD63 and tumor susceptibility gene 101 (TSG101) (Fig. 1C).

Vesicle-like structures were also observed in, and on, the syncitial tegument of *E. multilocularis* PSCs by TEM (Fig. 1D). Two different sizes were distinguished: smaller EVs with diameters ~70 nm, falling into the range of exosome-sized vesicles (Exo), and larger EVs with diameters of ~300nm, the range of microvesicles (MVs). Multivesicular bodies (MVBs) observed in the tegument had either a dense or an electron-lucent matrix surrounding intraluminal vesicles (ILVs) (Fig. 1D). Moreover, highly expressed tetraspanins were identified on the teguments of PSCs and the germinal layers of cysts (Fig. 1E) in liver sections containing metacestodes from mice infected with *E. multilocularis*. These findings suggest that the PSC tegument and cyst germinal layer may be involved in the formation and recycling of EVs.

2. 2 Parasite and host-derived proteins in E. multilocularis *EVs*

Proteomic analysis was used to characterize the protein composition of *E. multilocularis* EVs. Thousands of parasite-derived proteins and hundreds of host (mouse)-derived proteins were identified in 30 µg *E. multilocularis* EVs, PSCs culture medium and whole PSCs lysis (Fig. 2A, Table S01-03). Despite considerable concordance between the different isolates, it was striking that the EV composition was highly distinct from whole parasite lysates and PSCs culture medium. In total, 1082 parasites proteins were identified in PSCs culture medium and 1407 proteins in EVs released by PSCs. Of these proteins, 263 were identified exclusively in PSCs culture medium and 588 only in EVs (Fig. 2A). Among these, several exosomal markers, including heat shock protein 70 (HSP70), TSG101, tetraspanins, 14-3-3 and enolase were identified in *E. multilocularis* PSCs EVs (Table 1, Table S01). Because parasites were cultured with FBS before collecting EVs, bovine proteins were also present in purified EVs, including polyubiquitin-C, actin, myosin heavy chain 9 and so on (Table1, Fig. S02 and Table S03). However, host (mouse)-derived proteins identified in *E. multilocularis* PSCs EVs were more diverse than bovine-derived proteins, and many were annotated as associated with the immune response (Table 1, Table S04).

GO analysis of those proteins exclusively identified in EVs indicates that parasite-derived proteins associated with vesicle targeting and exocytosis are overrepresented, indicating exocytic vesicle origin, while host-derived proteins were mostly related to actin filament fragmentation and other biological processes (Fig. 2B). Meanwhile, parasite-derived proteins in EVs were enriched in endocytosis pathway components (Fig. 2C), indicating that these EVs are exosomes derived from endosomal structures (Fig. 2D). However, the mouse-derived proteins in *E. multilocularis* PSCs EVs were closely associated with immune response and focal adhesion, and hence potentially promoting angiogenesis (Fig. 2C and 2D).

2.3 Comparative analysis of EV protein cargo between cestode species

Cestode EVs are an important component in host-parasite interactions, and proteins enriched in EVs are hence candidate effector molecules. To systematically compare parasite- and host-derived proteins in EVs released by different cestode species protein domain classification for all available proteomic datasets was performed (Table S04-05). Interestingly, the majority of domains in parasite-derived EV proteins appear to be species-specific, with only three parasite-derived domains common to all cestode datasets (seven species in total), including Rab11-like, C2 superfamily and annexin, all of which are domains possessed by classical EVs marker proteins (Fig. 3A and 3C, Fig. S03 and Table S04). Only two host-derived domains, IgC1L and Ig superfamily, were common to all four species, both of which are associated with the immune response (Fig. 3B and 3D). As many as 670 parasite-derived domains and 119 host-derived domains are shared between *E. multilocularis* and *E. granulosus* EV proteomes (Table S05-06). Hence, the common parasite proteins present in these EVs may serve as markers for validating cestode or *Echinococcus* spp. EVs, such as tetraspanin family proteins, major egg antigen p40 and tegumental antigen, immunoglobulin-like proteins, proteins involved in vesicle trafficking (Rabs, Ubiquitin E3, SNAREs, TSG101, Alix), transporters and channels, structural proteins and others, although the EV proteins in the reported datasets are diverse (Fig. 3E). To discriminate for parasite-specific proteins, species-specific antibodies or mass spectrometric detection are required. However, the enriched proteins derived from host identified in *E. granulosus* PSC EVs and other cestode EVs reported by other studies were not related to the focal adhesion pathway, indicating that this pathway is potentially species-specific.

2.4 Extracellular vesicles from the E. multilocularis *protoscolex induce HUVEC proliferation and tube formation*

Given that development of *Echinococcus* spp. in mammalian hosts is associated with formation of new permeable blood vessels, a protein angiogenesis array was used to analyse tissue lysates obtained from *Echinococcus*-infected and uninfected mice livers. Compared to uninfected mice, *Echinococcus*-infected livers had increased levels of multiple angiogenesis regulating molecules, including VEGF, matrix metallopeptidase 9 (MMP9), monocyte chemoattractant protein-1 (MCP-1), stromal cell derived factor 1 (SDF-1), and serpin E1 (plasminogen activator inhibitor-1 (Fig. 4A). Angiogenic stimulation in *E. multilocularis*-infected mice was confirmed by immunohistochemical analysis, with the number of CD31+ vessels and VEGF expression levels significantly increased in the livers of infected mice (Fig. 4B).

The impact of *E. multilocularis* PSCs EVs on endothelial cells was further examined by a tube-formation assay using HUVECs. The length of HUVEC tubes treated with EVs significantly increased compared to those incubated with DMEM alone or PSC culture medium, while whole PSC lysates significantly disturbed HUVEC tube formation (Fig. 4C). Proliferation of HUVECs was also significantly promoted by EVs shed from PSCs after 48 hrs (Fig. 4D). These data demonstrate that *E. multilocularis* EVs may contribute to the augmented angiogenesis observed in the livers of *E. multilocularis*-infected mice (Fig. 5).

3. Discussion

EVs released from *E. multilocularis* PSCs contain abundant materials derived from both parasite and host, and can potentially regulate parasite-parasite and parasite-host interactions. Unlike *E. granulosus,* which presents a typical unilocular, subspherical cyst that grows by concentric enlargement*,* the *E. multilocularis* metacestode is a multivesicular, infiltrating structure with no obvious limiting host-tissue barrier [3, 4]. Proliferation of *E. multilocularis* metacestode occurs both endogenously and exogeneously and is attributable to the undifferentiated cells of the germinal layer, leading to the production of numerous PSCs and cysts that can directly contact with host tissues [3, 4]. Hence, the contents of the *E. multilocularis* metacesotde, typically germinal cells and PSCs, are potentially more able to interact with host cells and participate in regulation of host-parasite interactions, comparing to *E. granulosus* cysts.

To understand the molecular basis for interactions between parasite and host, we analysed the EVs released by *E. multilocularis* PSCs, and characterized their protein composition and roles in regulating host cells and tissues. Two major EV classes, namely Exo and MVs, both of which can participate in cell-cell communication [7], potentially derived from endocytic compartments and plasma membrane budding respectively, were shed from the *E. multilocularis* tegument observed under TEM. Proteomics was fully consistent with the Exo as the most abundant EVs in the present study, as proteins associated with the endomembrane system were enriched in the EVs released from *E. multilocularis* PSCs. Furthermore, these findings indicate that EV biogenesis in *E. multilocularis* is broadly conserved with mammalian and other parasites [21]. Among the identified EV proteins, tetraspanins and TSG101, enriched in E. *multilocularis* PSCs EVs, are candidates for development as EVs markers.

Biogenesis of EVs proceeds *via* an endolysosomal pathway with inward budding of the plasma membrane generating an endosome, which in turn fuses with cargo-containing endocytic vesicles. Endosomal membrane further buds inward to form intraluminal vesicles within MVBs, which fuse with the plasma membrane, releasing these vesicles as EVs [9], and likely involves both ESCRT-dependent and ESCRT-independent pathways. For example, ESCRT components including hepatocyte growth factor-regulated tyrosine kinase substrate (HRS), signal transducing adaptor molecule 1 (STAM1), TSG101, ESCRT accessory protein ALIX and the others [39], were identified in PSC EVs. For ESCRT-independent pathways, tetraspanins also play crucial roles in sorting of multiple proteins, such as the luminal domain of premelanosome protein [40]. Hence, the abundant tetraspanins recovered in *E. multilocularis* EVs point to potential roles for EV ESCRT-independent biogenesis.

Host-derived macromolecules, including proteins and miRNAs, have been reported in EVs released by cestodes [21, 24, 34] and intracellular parasites [8, 9]. The most abundant host-derived proteins in EVs were immunoglobulins and complement factors [34], and were also identified here, rather than as bovine derived proteins Under TEM, EVs from the tegument of *E. multilocularis* were observed resembling EVs released from other platyhelminths [34, 42]. In addition, there was evidence that host IgG deposited in the tegument of *E. ortleppi* [41]. Hence, the presence of host immunoglobulins in these parasites indicates that they may be packed into the membranes of parasite EVs during releasing into the extracellular space, and involve in the regulation of host-parasite interaction [34, 42]. Importantly, KEGG analysis revealed that some pathways, including focal adhesion, were enriched in *E. multilocularis* EVs, suggesting a possible angiogenesis-promoting mechanism.

High expression of pro-angiogenic factors in the liver of mice infected with *E. multilocularis* together with previous studies [27-30], underscore the ability of *E. multilocularis* to mediate neovascularization. Analogous to an aggressive tumor, *E. multilocularis* is invasive and causes pathological angiogenesis to provide nutrients and metabolite excretion for parasite growth, maturation and invasion. However, mechanisms underpinning these phenomena are poorly understood. A multifactorial induction of parasite-associated neovascularization could arise through host-, parasite- or host- plus parasite-dependent angiogenic mechanisms [43]. An emerging paradigm is that EVs transfer helminth molecules to HUVECs, participate in blood clot modulation, vasodilation and vascular smooth muscle contraction exemplified by *Schistosoma* [44], and *Leishmania* [45]. Furthermore, exosomes are important messengers between tumor cells and vascular endothelial cells in hypoxia-driven pro-angiogenic tumor responses, frequently mediated by miRNAs, such as miR-21-5p, miR-30b, miR-100 and others [16, 23-25]. However, analogs to these miRNAs are absent from EVs released by *Echinococcus* spp [16, 23-25]. Regardless, we found that *E. multilocularis* PSCs can promote HUVEC proliferation and tube formation through shedding EVs, potentially inducing angiogenesis via related proteins packaged into EVs. However, we cannot exclude impacts from EV-derived miRNAs mediating physiological changes, as exemplified by HUVECs.

Parasite EVs can directly interact with multiple cells in infected hosts and has been extensively characterised in dendritic cells, macrophages, T cells and B cells [46].

These cells exert direct effects on parasites or recipient cells by targeted immunomodulatory strategies to maintain homeostasis, including suppression of type 1 responses, stimulation of Th1- or Th2-responses and induction of type 2 tolerogeneic phenotypes [46]. We identified many proteins in EVs with potential immunological impact. For example, the 14-3-3 protein played vital roles in regulation of inflammatory responses and immunization with recombinant *E. multilocularis* 14-3-3 protein provided 97% protection against a *E. multilocularis* challenge infection [47], HSP70 proteins activated inflammatory pathways [48], cathepsins interacted with macrophages and led to suppression of Th1 responses [48], integrins were involved in activating TGFβ1 to control immune homeostasis [49] and annexin (also found as a host-derived protein here) had the capacity to bind and activate host plasminogen, suggesting a role in parasite invasion [22]. In addition to components commonly found in exosomes generated by most cell types, a series of parasite-specific virulence factors were among the most abundant proteins in the exosomal proteome, such as HSPs and highly immunogenic and tolerogenic antigens. These antigens potentially modulate host defense by suppressing neutrophils and dendritic cell-mediated innate responses and T cell-dependent mechanisms, and influencing the intensity and quality of the global adaptive immune response [21].

In conclusion, we provide deeper understanding of the protein composition of EVs released by *E. multilocularis* PSCs. Both ESCRT-dependent and -independent pathways are involved in the biogenesis of *E. multilocularis* EVs. Moreover, EVs from both parasite and host potentially play important roles in manipulating host development and parasite survival as well as the resulting pathology. It is likely that EVs of multiple cellular origin are involved in vascular development, growth and maturation [50]. In addition, our study indicates that host-derived proteins in EVs released by the parasite are key players to angiogenesis, promoting HUVEC proliferation and tube formation. However, further exploration of the functions of *E. multilocularis* EVs is required to elucidate the precise mechanisms related to angiogenesis and other interactions between the host and *E. multilocularis*.

Conflict of interest statement

The authors declare that the research was conducted in the absence of any commercial or financial relationships that could be construed as a potential conflict of interest.

Author contributions

Jianhai Yin, Jianping Cao and Congshan Liu designed and supervised the whole project. Congshan Liu and Jianhai Yin performed experiments, collected, analyzed, and interpreted data. Congshan Liu, Mark C. Field and Jianhai Yin drafted the manuscript and participated in the preparation of its final version. Jianping Cao, Haobing Zhang and Mark C. Field participated in revision and the final version of the manuscript.

Funding information

This study was funded by National Natural Science Foundation of China (Award number 81702030 to JHY), Natural Science Foundation of Shanghai (Award number 20ZR1463600 to CSL)and the Wellcome Trust (Award number 204697/Z/16/Z to

MCF).

Data availability statement

The data that support the findings of this study are available in the methods and/or supplementary material of this article. The mass spectrometry proteomics data have been deposited to the ProteomeXchange Consortium via the iProX partner repository with the dataset identifier PXD035601.

Appendix A. Supplementary data

Supplementary data to this article can be found online at

REFERENCES

[1] Eckert J, Deplazes P. Biological, epidemiological, and clinical aspects of echinococcosis, a zoonosis of increasing concern. Clinical microbiology reviews 2004;17:107-35.https://10.1128/CMR.17.1.107-135.2004.
[2] Deplazes P, Rinaldi L, Alvarez Rojas CA, Torgerson PR, Harandi MF, Romig T, et al. Global Distribution of Alveolar and Cystic Echinococcosis. Advances in parasitology 2017;95:315-493.https://10.1016/bs.apar.2016.11.001.
[3] Moro P, Schantz PM. Echinococcosis: a review. International journal of infectious diseases : IJID : official publication of the International Society for Infectious Diseases 2009;13:125-33.https://10.1016/j.ijid.2008.03.037.
[4] Thompson RC. Biology and Systematics of Echinococcus. Advances in parasitology 2017;95:65-109.https://10.1016/bs.apar.2016.07.001.
[5] Kalluri R, LeBleu VS. The biology, function, and biomedical applications of exosomes. Science 2020;367.https://10.1126/science.aau6977.
[6] Cocucci E, Meldolesi J. Ectosomes and exosomes: shedding the confusion between extracellular vesicles. Trends in cell biology 2015;25:364-72.https://10.1016/j.tcb.2015.01.004.
[7] Gurung S, Perocheau D, Touramanidou L, Baruteau J. The exosome journey: from biogenesis to uptake and intracellular signalling. Cell communication and signaling : CCS 2021;19:47.https://10.1186/s12964-021-00730-1.
[8] Ofir-Birin Y, Regev-Rudzki N. Extracellular vesicles in parasite survival. Science 2019;363:817-8.https://10.1126/science.aau4666.
[9] Mardahl M, Borup A, Nejsum P. A new level of complexity in parasite-host interaction: The role of extracellular vesicles. Advances in parasitology 2019;104:39-112.https://10.1016/bs.apar.2019.02.003.
[10] Silverman JM, Clos J, de'Oliveira CC, Shirvani O, Fang Y, Wang C, et al. An exosome-based secretion pathway is responsible for protein export from Leishmania and communication with macrophages. Journal of cell science 2010;123:842-52.https://10.1242/jcs.056465.
[11] Sisquella X, Ofir-Birin Y, Pimentel MA, Cheng L, Abou Karam P, Sampaio NG, et al. Malaria parasite DNA-harbouring vesicles activate cytosolic immune sensors. Nature communications 2017;8:1985.https://10.1038/s41467-017-02083-1.
[12] Nicolao MC, Rodriguez Rodrigues C, Cumino AC. Extracellular vesicles from Echinococcus granulosus larval stage: Isolation, characterization and uptake by dendritic cells. PLoS neglected tropical diseases 2019;13:e0007032.https://10.1371/journal.pntd.0007032.
[13] Brehm K, Koziol U. Echinococcus-Host Interactions at Cellular and Molecular Levels. Advances in parasitology 2017;95:147-212.https://10.1016/bs.apar.2016.09.001.
[14] Gottstein B, Soboslay P, Ortona E, Wang J, Siracusano A, Vuitton D. Immunology of Alveolar and Cystic Echinococcosis (AE and CE). Advances in parasitology 2017;96:1-54.https://10.1016/bs.apar.2016.09.005.
[15] Grubor NM, Jovanova-Nesic KD, Shoenfeld Y. Liver cystic echinococcosis and human host immune and autoimmune follow-up: A review. World journal of hepatology 2017;9:1176-89.https://10.4254/wjh.v9.i30.1176.
[16] Yang J, Wu J, Fu Y, Yan L, Li Y, Guo X, et al. Identification of Different Extracellular Vesicles in the Hydatid Fluid of Echinococcus granulosus and Immunomodulatory Effects of 110 K EVs on Sheep

PBMCs. Frontiers in immunology 2021;12:602717.https://10.3389/fimmu.2021.602717.
[17] Zheng Y, Guo X, Su M, Guo A, Ding J, Yang J, et al. Regulatory effects of Echinococcus multilocularis extracellular vesicles on RAW264.7 macrophages. Veterinary parasitology 2017;235:29-36.https://10.1016/j.vetpar.2017.01.012.
[18] Zhou X, Wang W, Cui F, Shi C, Ma Y, Yu Y, et al. Extracellular vesicles derived from Echinococcus granulosus hydatid cyst fluid from patients: isolation, characterization and evaluation of immunomodulatory functions on T cells. International journal for parasitology 2019;49:1029-37.https://10.1016/j.ijpara.2019.08.003.
[19] Jeong MJ, Kang SA, Choi JH, Lee DI, Yu HS. Extracellular vesicles of Echinococcus granulosus have therapeutic effects in allergic airway inflammation. Parasite immunology 2021;43:e12872.https://10.1111/pim.12872.
[20] Zheng Y, Guo X, Su M, Chen X, Jin X, Ding J, et al. Identification of emu-TegP11, an EF-hand domain-containing tegumental protein of Echinococcus multilocularis. Veterinary parasitology 2018;255:107-13.https://10.1016/j.vetpar.2018.04.006.
[21] Siles-Lucas M, Sanchez-Ovejero C, Gonzalez-Sanchez M, Gonzalez E, Falcon-Perez JM, Boufana B, et al. Isolation and characterization of exosomes derived from fertile sheep hydatid cysts. Veterinary parasitology 2017;236:22-33.https://10.1016/j.vetpar.2017.01.022.
[22] Wu J, Cai M, Yang J, Li Y, Ding J, Kandil OM, et al. Comparative analysis of different extracellular vesicles secreted by Echinococcus granulosus protoscoleces. Acta tropica 2021;213:105756.https://10.1016/j.actatropica.2020.105756.
[23] Zhang X, Gong W, Cao S, Yin J, Zhang J, Cao J, et al. Comprehensive Analysis of Non-coding RNA Profiles of Exosome-Like Vesicles From the Protoscoleces and Hydatid Cyst Fluid of Echinococcus granulosus. Frontiers in cellular and infection microbiology 2020;10:316.https://10.3389/fcimb.2020.00316.
[24] Ancarola ME, Lichtenstein G, Herbig J, Holroyd N, Mariconti M, Brunetti E, et al. Extracellular non-coding RNA signatures of the metacestode stage of Echinococcus multilocularis. PLoS neglected tropical diseases 2020;14:e0008890.https://10.1371/journal.pntd.0008890.
[25] Ding J, He G, Wu J, Yang J, Guo X, Yang X, et al. miRNA-seq of Echinococcus multilocularis Extracellular Vesicles and Immunomodulatory Effects of miR-4989. Frontiers in microbiology 2019;10:2707.https://10.3389/fmicb.2019.02707.
[26] Cai M, Ding J, Li Y, He G, Yang J, Liu T, et al. Echinococcus multilocularis infection induces UBE2N suppression via exosomal emu-miR-4989. Acta tropica 2021;223:106087.https://10.1016/j.actatropica.2021.106087.
[27] Jian-Hai Y, Yu-Juan S, Ai-Ping Y, Jian-Ping C. [In vitro pro - angiogenic activity of Echinococcus granulosus hydatid cysts from experimentally infected mice]. Zhongguo xue xi chong bing fang zhi za zhi = Chinese journal of schistosomiasis control 2017;29:320-3.https://10.16250/j.32.1374.2017052.
[28] Yin J, Shen Y, Yu A, Liu C, Yao J, Gong W, et al. The proangiogenic role of polymorphonuclear myeloid-derived suppressor cells in mice infected with Echinococcus granulosus. Bioscience trends 2018;12:338-41.https://10.5582/bst.2018.01105.
[29] Jiang HJ, Gui XW, GUO LJ, Yang XF, Wang XY, Chen XL, et al. Expression and angiogenic effect of VEGFA/VEGFR2 in mice hepatic metacestode tissue of Echinococcus multilocularis. Zhongguo ji sheng chong xue yu ji sheng chong bing za zhi = Chinese journal of parasitology & parasitic diseases 2020;38.https://10.12140/j.issn.1000-7423.2020.06.001.
[30] Qing Z, Yang XF, Han HH, GUO LJ, Jiang HJ, Wang XY, et al. Correlation between angiogenesis and disease progression of hepatic Echinococcus multilocularis in C57BL/6 mice. Zhongguo ji sheng chong xue yu ji sheng chong bing za zhi = Chinese journal of parasitology & parasitic diseases 2019;37.https://10.12140/j.issn.1000-7423.2019.03.011.
[31] Liu C, Yin J, Yao J, Xu Z, Tao Y, Zhang H. Pharmacophore-Based Virtual Screening Toward the Discovery of Novel Anti-echinococcal Compounds. Frontiers in cellular and infection microbiology 2020;10:118.https://10.3389/fcimb.2020.00118.
[32] Schneider CA, Rasband WS, Eliceiri KW. NIH Image to ImageJ: 25 years of image analysis. Nature methods 2012;9:671-5.https://10.1038/nmeth.2089.
[33] Shi C, Zhou X, Yang W, Wu J, Bai M, Zhang Y, et al. Proteomic Analysis of Plasma-Derived Extracellular Vesicles From Mice With Echinococcus granulosus at Different Infection Stages and Their Immunomodulatory Functions. Frontiers in cellular and infection microbiology 2022;12:805010.https://10.3389/fcimb.2022.805010.
[34] Ancarola ME, Marcilla A, Herz M, Macchiaroli N, Perez M, Asurmendi S, et al. Cestode parasites

release extracellular vesicles with microRNAs and immunodiagnostic protein cargo. International journal for parasitology 2017;47:675-86.https://10.1016/j.ijpara.2017.05.003.
[35] Wang LQ, Liu TL, Liang PH, Zhang SH, Li TS, Li YP, et al. Characterization of exosome-like vesicles derived from Taenia pisiformis cysticercus and their immunoregulatory role on macrophages. Parasites & vectors 2020;13:318.https://10.1186/s13071-020-04186-z.
[36] Mazanec H, Konik P, Gardian Z, Kuchta R. Extracellular vesicles secreted by model tapeworm Hymenolepis diminuta: biogenesis, ultrastructure and protein composition. International journal for parasitology 2021;51:327-32.https://10.1016/j.ijpara.2020.09.010.
[37] Liang P, Mao L, Zhang S, Guo X, Liu G, Wang L, et al. Identification and molecular characterization of exosome-like vesicles derived from the Taenia asiatica adult worm. Acta tropica 2019;198:105036.https://10.1016/j.actatropica.2019.05.027.
[38] Conway JR, Lex A, Gehlenborg N. UpSetR: an R package for the visualization of intersecting sets and their properties. Bioinformatics 2017;33:2938-40.https://10.1093/bioinformatics/btx364.
[39] Kang T, Atukorala I, Mathivanan S. Biogenesis of Extracellular Vesicles. Sub-cellular biochemistry 2021;97:19-43.https://10.1007/978-3-030-67171-6_2.
[40] van Niel G, Charrin S, Simoes S, Romao M, Rochin L, Saftig P, et al. The tetraspanin CD63 regulates ESCRT-independent and -dependent endosomal sorting during melanogenesis. Developmental cell 2011;21:708-21.https://10.1016/j.devcel.2011.08.019.
[41] Miles S, Magnone J, Garcia-Luna J, Ancarola ME, Cucher M, Dematteis S, et al. Ultrastructural characterization of the tegument in protoscoleces of Echinococcus ortleppi. International journal for parasitology 2021;51:989-97.https://10.1016/j.ijpara.2021.05.004.
[42] Kifle DW, Pearson MS, Becker L, Pickering D, Loukas A, Sotillo J. Proteomic analysis of two populations of Schistosoma mansoni-derived extracellular vesicles: 15k pellet and 120k pellet vesicles. Molecular and biochemical parasitology 2020;236:111264.https://10.1016/j.molbiopara.2020.111264.
[43] Dennis RD, Schubert U, Bauer C. Angiogenesis and parasitic helminth-associated neovascularization. Parasitology 2011;138:426-39.https://10.1017/S0031182010001642.
[44] Kifle DW, Chaiyadet S, Waardenberg AJ, Wise I, Cooper M, Becker L, et al. Uptake of Schistosoma mansoni extracellular vesicles by human endothelial and monocytic cell lines and impact on vascular endothelial cell gene expression. International journal for parasitology 2020;50:685-96.https://10.1016/j.ijpara.2020.05.005.
[45] Gioseffi A, Hamerly T, Van K, Zhang N, Dinglasan RR, Yates PA, et al. Leishmania-infected macrophages release extracellular vesicles that can promote lesion development. Life science alliance 2020;3.https://10.26508/lsa.202000742.
[46] Eichenberger RM, Sotillo J, Loukas A. Immunobiology of parasitic worm extracellular vesicles. Immunology and cell biology 2018.https://10.1111/imcb.12171.
[47] Siles-Lucas M, Merli M, Mackenstedt U, Gottstein B. The Echinococcus multilocularis 14-3-3 protein protects mice against primary but not secondary alveolar echinococcosis. Vaccine 2003;21:431-9.https://10.1016/s0264-410x(02)00517-0.
[48] Robinson MW, Hutchinson AT, Donnelly S, Dalton JP. Worm secretory molecules are causing alarm. Trends in parasitology 2010;26:371-2.https://10.1016/j.pt.2010.05.004.
[49] Worthington JJ, Fenton TM, Czajkowska BI, Klementowicz JE, Travis MA. Regulation of TGFbeta in the immune system: an emerging role for integrins and dendritic cells. Immunobiology 2012;217:1259-65.https://10.1016/j.imbio.2012.06.009.
[50] Szempruch AJ, Sykes SE, Kieft R, Dennison L, Becker AC, Gartrell A, et al. Extracellular Vesicles from Trypanosoma brucei Mediate Virulence Factor Transfer and Cause Host Anemia. Cell 2016;164:246-57.https://10.1016/j.cell.2015.11.051.

Figure legends

Fig. 1. Characterization of extracellular vesicles secreted by *E. multilocularis* protoscoleces. A) Morphological characterization of purified EVs by TEM. B) Size distribution of isolated EVs determined by TEM. C. Western blot analysis of EV markers, CD63 and TSG101 in *E. multilocularis* PSC lysis and EVs (10 μg total protein). D) TEM of *E. multilocularis* tegument releasing EVs (Exo, exosome; MVs, microvesicles; MVB, multivesicular body). E) Localisation of *E. multilocularis* tetraspanin CD63 in metacestodes (G: germinal layer; T: tegument).

Fig. 2. Profiles of proteins identified in EVs released by *E. multilocularis* PSCs. A) Numbers of parasite and host derived proteins identified in *E. multilocularis* PSC lysis, PSCs culture medium and EVs released by PSCs. B) GO analysis of parasite- and host-derived proteins exclusively identified in EVs released by *E. multilocularis* PSCs. C) KEGG clusters of parasite- and host-derived proteins exclusively identified in EVs released by *E. multilocularis* PSCs. Each node represented an enriched term, and the node color represented different clusters; the node size represented six levels of enriched p-value, node size from small to large: [0.05, 1], [0.01, 0.05), [0.001, 0.01), [0.0001, 0.001), [1e-10, 0.0001), [0, 1e-10). D) KEGG pathway of *E. multilocularis* endocytosis and mouse focal adhesion EV-associated proteins. Red, proteins exclusively identified in EVs released by *E. multilocularis* PSCs; pink, proteins identified in EVs released by *E. multilocularis* PSCs and culture medium; green, proteins associated with pathway without corresponding proteins in EVs released by *E. multilocularis* PSCs; white, proteins reported to be associated with this pathway but absent from the *E. multilocularis* genome.

Fig. 3. Protein representation between EVs of multiple-species. A) UpSetR analysis visualizing intersections between unique conserved domains of parasite-derived proteins found in cestodes extracellular vesicles (EVs). The same color indicated that data was retrieved from the same study. B) UpSetR analysis visualizing intersections between unique conserved domains of host-derived proteins found in cestodes EVs. Intersecting datasets are shown as filled circles; the corresponding number of domains in that intersection is presented on top of each histogram. The set size represents the number of domains found in each dataset. C) Conserved domain distribution of parasite-derived proteins in available cestode EVs-contained datasets. The same color indicated that data was retrieved from the same study. D) Conserved domain distribution of host-derived proteins in available cestode EVs-contained datasets (Dark grey, presence; light grey, absence). E. Schematic representation of proteins and domains in EVs shed by *Echinococcus* spp (Black: parasite-derived proteins; Red: host-derived proteins; Purple: parasite- and host-derived common proteins). Please find the complete list of domain information in Table S04-05.

Fig. 4. Angiogenesis induced by *E. multilocularis* infection and EVs released by *E. multilocularis* PSCs. A) The Mouse Angiogenesis Array detected multiple analytes in tissue lysates. A total of 300 μg of tissue lysate was run on each array (n=3). Factors with fold change (infected/normal) >=2 are called out. B) Immunohistochemical detection of CD31 and VEGF in liver tissues of *E. multilocularis*-infected and non-infected mice. C) Tube formation of HUVECs after incubation with *E. multilocularis* PSC culture medium (10 μg), EVs (10 μg) and whole PSC lysis (10 μg). D) Effects of *E. multilocularis* materials (10 μg) on HUVEC proliferation.

Fig. 5. Model for *E. multilocularis* PSCs EVs and host EVs involvement in angiogenesis. *E. multilocularis* lesions are mostly located in host livers, where immune, fibroblast and vascular cells encyst the *E. multilocularis* metacestode containing invaginated and evaginated PSCs. Host cells and PSCs can release EVs into the lesion environment to regulate host-parasite interactions. Parasite EVs (orange) released by *E. multilocularis* PSCs and cysts can be internalized by various host cells, while host cells may also release EVs (blue) to regulate development of parasites. In addition, communication between host cells can also be facilitated by EVs.

Table legends

TABLE 1 Top 20 parasite and host-derived proteins exclusively identified in EVs released by *E. multilocularis* PSCs

Protein ID	Origins	Protein names
Q6VXZ5	*E.multilocularis*	Antigen B subunit 1
A0A068Y074	*E.multilocularis*	Polyubiquitin
A0A068YF78	*E.multilocularis*	Diagnostic antigen gp50
U6HHP6	*E.multilocularis*	Histone H2A
D9J2I8	*E.multilocularis*	Antigen B subunit 3
A0A068XWT9	*E.multilocularis*	Histone H2B
A0A068YDL3	*E.multilocularis*	Telomerase protein component 1
A0A087W0K1	*E.multilocularis*	Dynein light chain
A0A087VYL1	*E.multilocularis*	Expressed conserved protein
A0A068Y8K3	*E.multilocularis*	Ubiquitin modifier activating enzyme 1
A0A068YEV5	*E.multilocularis*	FERM central domain
A0A087W2S3	*E.multilocularis*	fructose-bisphosphatase
A0A068Y336	*E.multilocularis*	Tumor susceptibility locus tag 101 protein
A0A068YJ32	*E.multilocularis*	Ras protein rab
A0A087W1M1	*E.multilocularis*	Ras protein Rab 7a
A0A068Y3A1	*E.multilocularis*	Golgi-associated plant patholocus tagsis
Q24895	*E.multilocularis*	Endoplasmic reticulum chaperone BiP
U6I232	*E.multilocularis*	Tetraspanin
A0A068Y0X1	*E.multilocularis*	Tegumental antigen
A0A068Y706	*E.multilocularis*	Serine/threonine-protein phosphatase
Q6RFG4	*Mus musculus*	Myeloperoxidase
Q8C196	*Mus musculus*	Carbamoyl-phosphate synthase
Q99LC4	*Mus musculus*	Igh protein*
P13020	*Mus musculus*	Gelsolin*
Q3TWJ4	*Mus musculus*	Actin-related protein 3
Q9CVB6	*Mus musculus*	Actin-related protein 2/3 complex subunit 2
P68134	*Mus musculus*	Actin, alpha skeletal muscle
Q9DAC2	*Mus musculus*	Complement component C8 gamma chain*
Q542I3	*Mus musculus*	Pentaxin (Pentraxin)

A0A140T8P5	*Mus musculus*	Immunoglobulin kappa chain variable 8-24*
Q91Z25	*Mus musculus*	Actin-related protein 2/3 complex subunit
Q542I8	*Mus musculus*	Integrin beta*
Q3THX5	*Mus musculus*	Major vault protein
P50543	*Mus musculus*	Protein S100-A11
P40142	*Mus musculus*	Transketolase
P51437	*Mus musculus*	Cathelicidin antimicrobial peptide*
A0A075B5V7	*Mus musculus*	Immunoglobulin heavy variable V1-43*
P68372	*Mus musculus*	Tubulin beta-4B chain
Q3UVJ2	*Mus musculus*	Adenylyl cyclase-associated protein
B2RUF9	*Mus musculus*	Olfm4 protein
P0CH28	*Bos taurus (Bovine)*	Polyubiquitin-C
P60712	*Bos taurus (Bovine)*	Actin
F1MQ37	*Bos taurus (Bovine)*	Myosin heavy chain 9
P00974	*Bos taurus (Bovine)*	Pancreatic trypsin inhibitor
E1BNA9	*Bos taurus (Bovine)*	Zinc finger ZZ-type and EF-hand domain containing 1
P04272	*Bos taurus (Bovine)*	Annexin A2rotein I) (p36)
P61585	*Bos taurus (Bovine)*	Transforming protein RhoA
G3N081	*Bos taurus (Bovine)*	Histone H4
A6QPT4	*Bos taurus (Bovine)*	MPO protein
Q5E947	*Bos taurus (Bovine)*	Peroxiredoxin-1
P0CB32	*Bos taurus (Bovine)*	Heat shock 70 kDa protein 1-like
F1ML89	*Bos taurus (Bovine)*	Carbamoyl-phosphate synthase 1
F1N650	*Bos taurus (Bovine)*	Annexin
Q0VCX2	*Bos taurus (Bovine)*	Endoplasmic reticulum chaperone BiP
F1MWU9	*Bos taurus (Bovine)*	Heat shock protein family A (Hsp70) member 6
G3X757	*Bos taurus (Bovine)*	Transitional endoplasmic reticulum ATPase
P48616	*Bos taurus (Bovine)*	Vimentin
G3N0V2	*Bos taurus (Bovine)*	Keratin, type II cytoskeletal 1
P00760	*Bos taurus (Bovine)*	Serine protease 1
F1MAV0	*Bos taurus (Bovine)*	Fibrinogen beta chain

Proteins are listed by relative abundance.
* Immune response-related.

Supplementary materials:

Table S01 Parasite derived proteins in whole *E. multilocularis* protoscoleces lysates, *E. multilocularis* protoscoleces culture medium and EVs released by *E. multilocularis* protoscoleces.

Table S02 Host (mouse)-derived proteins in *E. multilocularis* protoscoleces lysates, *E. multilocularis* protoscoleces culture medium and EVs released by *E. multilocularis* protoscoleces.

Table S03 FBS derived proteins in whole *E. multilocularis* protoscoleces lysates, *E. multilocularis* protoscoleces culture medium and EVs released by *E. multilocularis* protoscoleces.

Table S04 Comparing the proteins in EVs released by *E. multilocularis* protoscoleces identified as mouse- and bovine-derived.

Table S05 Domains of parasite-derived EV proteins across several cestode species.

Table S06 Domains of host-derived EVs proteins across several cestode species.

Figure S01 Original images of size distribution determined by TEM.

Figure S02 Profiles of FBS (bovine)-derived proteins identified in EVs released by *E. multilocularis* PSCs. A) Numbers of. bovine-derived proteins (FBS) identified in *E. multilocularis* PSC lysis, PSCs culture medium and EVs released by PSCs. C) GO analysis of bovine-derived proteins exclusively identified in EVs released by *E. multilocularis* PSCs. B) KEGG clusters of bovine-derived proteins exclusively identified in EVs released by *E. multilocularis* PSCs. Each node represented an enriched term, and the node color represented different clusters; the node size represented six levels of enriched p-value, node size from small to large: [0.05, 1], [0.01, 0.05), [0.001, 0.01), [0.0001, 0.001), [1e-10, 0.0001), [0, 1e-10).

Figure S03 UpSetR analysis visualizing intersections between unique conserved domains of parasite-derived proteins found in cestodes extracellular vesicles (EVs). The same number in the sample name indicates that data were retrieved from the same study. Intersecting datasets are shown as filled circles, the corresponding number of domains in that intersection is presented on top of each histogram. The set size represents the number of domains found in each dataset.

Figure S04 Original images of the mouse angiogenesis array.

Figure S05 Original images of western blots.

protein ID	origins	Protein names
Q6VXZ5	*E.multilocularis*	Antigen B subunit 1
A0A068Y074	*E.multilocularis*	Polyubiquitin
A0A068YF78	*E.multilocularis*	Diagnostic antigen gp50
U6HHP6	*E.multilocularis*	Histone H2A
D9J2I8	*E.multilocularis*	Antigen B subunit 3
A0A068XWT9	*E.multilocularis*	Histone H2B
A0A068YDL3	*E.multilocularis*	Telomerase protein component 1
A0A087W0K1	*E.multilocularis*	Dynein light chain
A0A087VYL1	*E.multilocularis*	Expressed conserved protein
A0A068Y8K3	*E.multilocularis*	Ubiquitin modifier activating enzyme 1
A0A068YEV5	*E.multilocularis*	FERM central domain
A0A087W2S3	*E.multilocularis*	fructose-bisphosphatase
A0A068Y336	*E.multilocularis*	Tumor susceptibility locus tag 101 protein
A0A068YJ32	*E.multilocularis*	Ras protein rab
A0A087W1M1	*E.multilocularis*	Ras protein Rab 7a
A0A068Y3A1	*E.multilocularis*	Golgi associated plant patholocus tagsis
Q24895	*E.multilocularis*	Endoplasmic reticulum chaperone BiP
U6I232	*E.multilocularis*	Tetraspanin
A0A068Y0X1	*E.multilocularis*	Tegumental antigen
A0A068Y706	*E.multilocularis*	Serine/threonine-protein phosphatase
Q6RFG4	*Mus musculus*	Myeloperoxidase
Q8C196	*Mus musculus*	Carbamoyl-phosphate synthase
Q99LC4	*Mus musculus*	Igh protein*
P13020	*Mus musculus*	Gelsolin*
Q3TWJ4	*Mus musculus*	Actin-related protein 3
Q9CVB6	*Mus musculus*	Actin-related protein 2/3 complex subunit 2
P68134	*Mus musculus*	Actin, alpha skeletal muscle
Q9DAC2	*Mus musculus*	Complement component C8 gamma chain*
Q542I3	*Mus musculus*	Pentaxin (Pentraxin)
A0A140T8P5	*Mus musculus*	Immunoglobulin kappa chain variable 8-24*
Q91Z25	*Mus musculus*	Actin-related protein 2/3 complex subunit
Q542I8	*Mus musculus*	Integrin beta*
Q3THX5	*Mus musculus*	Major vault protein
P50543	*Mus musculus*	Protein S100-A11
P40142	*Mus musculus*	Transketolase
P51437	*Mus musculus*	Cathelicidin antimicrobial peptide*
A0A075B5V7	*Mus musculus*	Immunoglobulin heavy variable V1-43*
P68372	*Mus musculus*	Tubulin beta-4B chain
Q3UVJ2	*Mus musculus*	Adenylyl cyclase-associated protein
B2RUF9	*Mus musculus*	Olfm4 protein
P0CH28	*Bos taurus (Bovine)*	Polyubiquitin-C
P60712	*Bos taurus (Bovine)*	Actin
F1MQ37	*Bos taurus (Bovine)*	Myosin heavy chain 9
P00974	*Bos taurus (Bovine)*	Pancreatic trypsin inhibitor
E1BNA9	*Bos taurus (Bovine)*	Zinc finger ZZ-type and EF-hand domain containing 1

P04272	*Bos taurus (Bovine)*	Annexin A2rotein I) (p36)
P61585	*Bos taurus (Bovine)*	Transforming protein RhoA
G3N081	*Bos taurus (Bovine)*	Histone H4
A6QPT4	*Bos taurus (Bovine)*	MPO protein
Q5E947	*Bos taurus (Bovine)*	Peroxiredoxin-1
P0CB32	*Bos taurus (Bovine)*	Heat shock 70 kDa protein 1-like
F1ML89	*Bos taurus (Bovine)*	Carbamoyl-phosphate synthase 1
F1N650	*Bos taurus (Bovine)*	Annexin
Q0VCX2	*Bos taurus (Bovine)*	Endoplasmic reticulum chaperone BiP
F1MWU9	*Bos taurus (Bovine)*	Heat shock protein family A (Hsp70) member 6
G3X757	*Bos taurus (Bovine)*	Transitional endoplasmic reticulum ATPase
P48616	*Bos taurus (Bovine)*	Vimentin
G3N0V2	*Bos taurus (Bovine)*	Keratin, type II cytoskeletal 1
P00760	*Bos taurus (Bovine)*	Serine protease 1
F1MAV0	*Bos taurus (Bovine)*	Fibrinogen beta chain

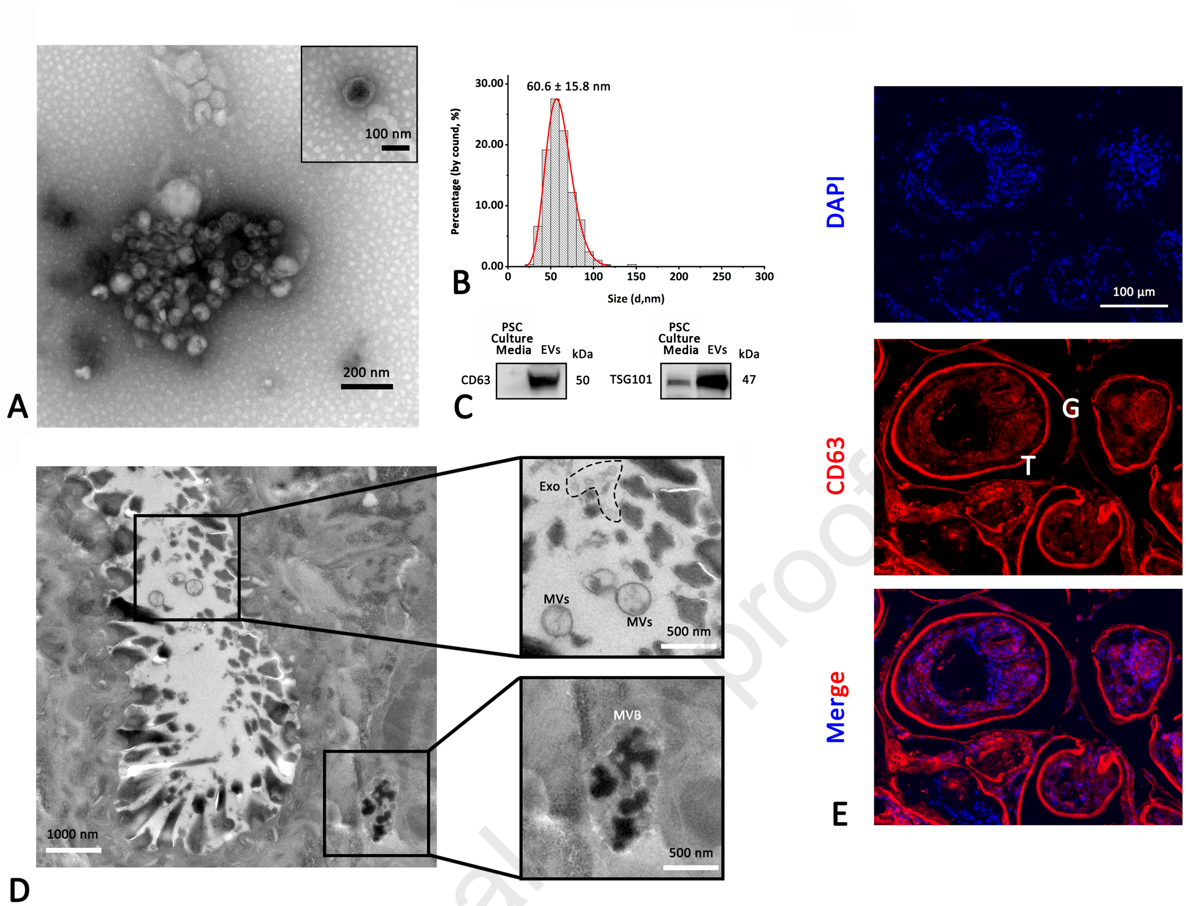
A
100 nm
200 nm
B
60.6 ± 15.8 nm
Percentage (by cound, %)
30.00
20.00
10.00
0.00
0
50
100
150
200
250
300
Size (d,nm)
C
PSC Culture Media
EVs
kDa
CD63
50
TSG101
47
D
1000 nm
Exo
MVs
500 nm
MVB
500 nm
DAPI
100 µm
CD63
G
T
Merge
E

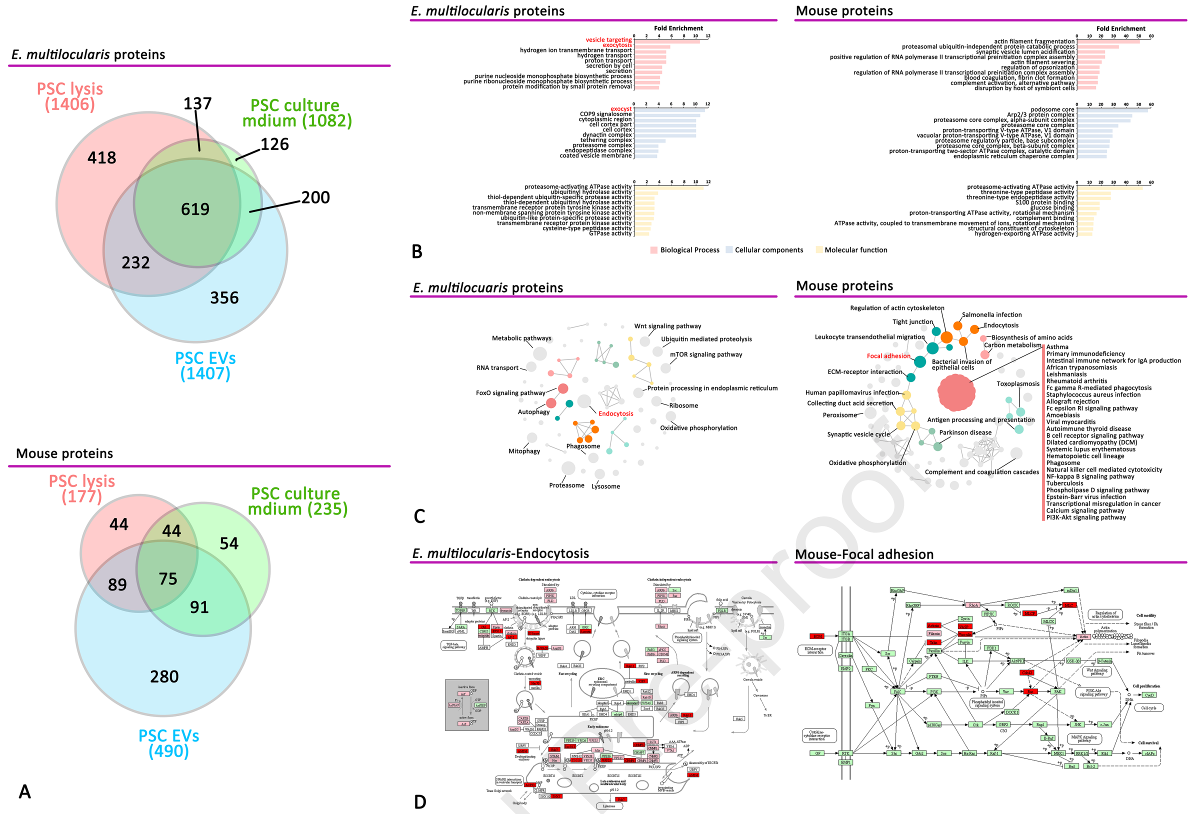
E. multilocularis proteins
PSC lysis (1406)
PSC culture mdium (1082)
PSC EVs (1407)
418
137
126
619
200
232
356
Mouse proteins
PSC lysis (177)
PSC culture mdium (235)
PSC EVs (490)
44
44
54
89
75
91
280
A
E. multilocularis proteins
Mouse proteins
Fold Enrichment
Biological Process
Cellular components
Molecular function
B
E. multilocuaris proteins
Mouse proteins
Endocytosis
Focal adhesion
C
E. multilocularis-Endocytosis
Mouse-Focal adhesion
D

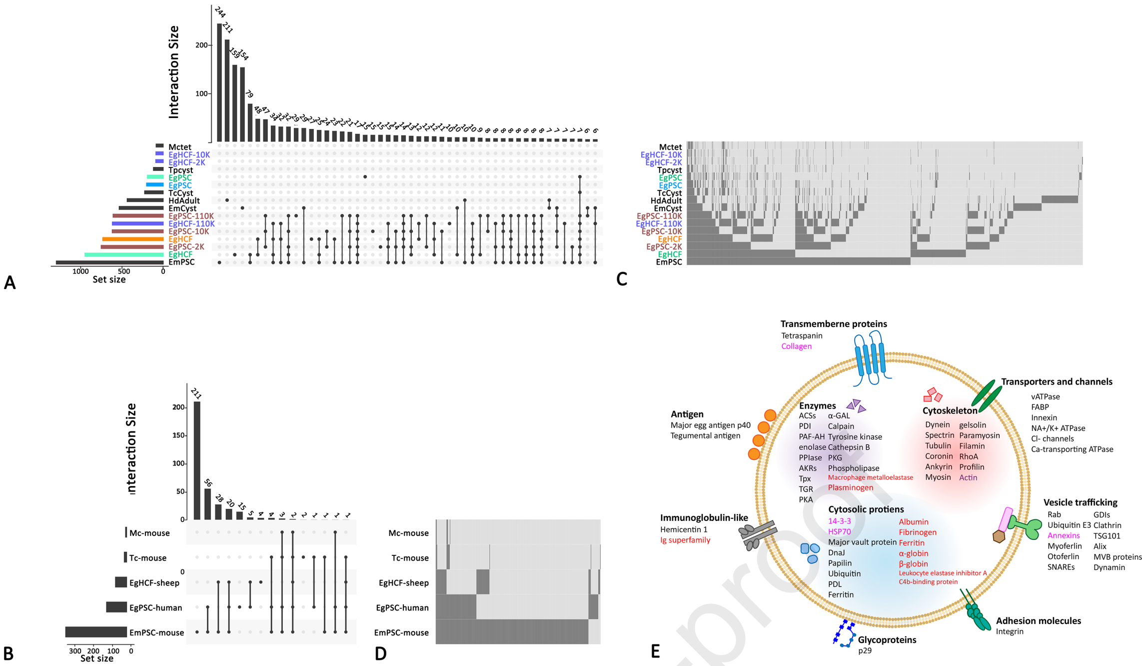

Interaction Size
Set size
Mctet
EgHCF-10K
EgHCF-2K
Tpcyst
EgPSC
EgPSC
TcCyst
HdAdult
EmCyst
EgPSC-110K
EgHCF-110K
EgPSC-10K
EgHCF
EgPSC-2K
EgHCF
EmPSC
A
C
Mc-mouse
Tc-mouse
EgHCF-sheep
EgPSC-human
EmPSC-mouse
B
D
Transmemberne proteins
Tetraspanin
Collagen
Transporters and channels
vATPase
FABP
Innexin
NA+/K+ ATPase
Cl- channels
Ca-transporting ATPase
Antigen
Major egg antigen p40
Tegumental antigen
Enzymes
ACSs α-GAL
PDI Calpain
PAF-AH Tyrosine kinase
enolase Cathepsin B
PPIase PKG
AKRs Phospholipase
Tpx Macrophage metalloelastase
TGR Plasminogen
PKA
Cytoskeleton
Dynein gelsolin
Spectrin Paramyosin
Tubulin Filamin
Coronin RhoA
Ankyrin Profilin
Myosin Actin
Immunoglobulin-like
Hemicentin 1
Ig superfamily
Cytosolic protiens
14-3-3
HSP70
Major vault protein
DnaJ
Papilin
Ubiquitin
PDL
Ferritin
Albumin
Fibrinogen
Ferritin
α-globin
β-globin
Leukocyte elastase inhibitor A
C4b-binding protein
Vesicle trafficking
Rab GDIs
Ubiquitin E3 Clathrin
Annexins TSG101
Myoferlin Alix
Otoferlin MVB proteins
SNAREs Dynamin
Adhesion molecules
Integrin
Glycoproteins
p29
E

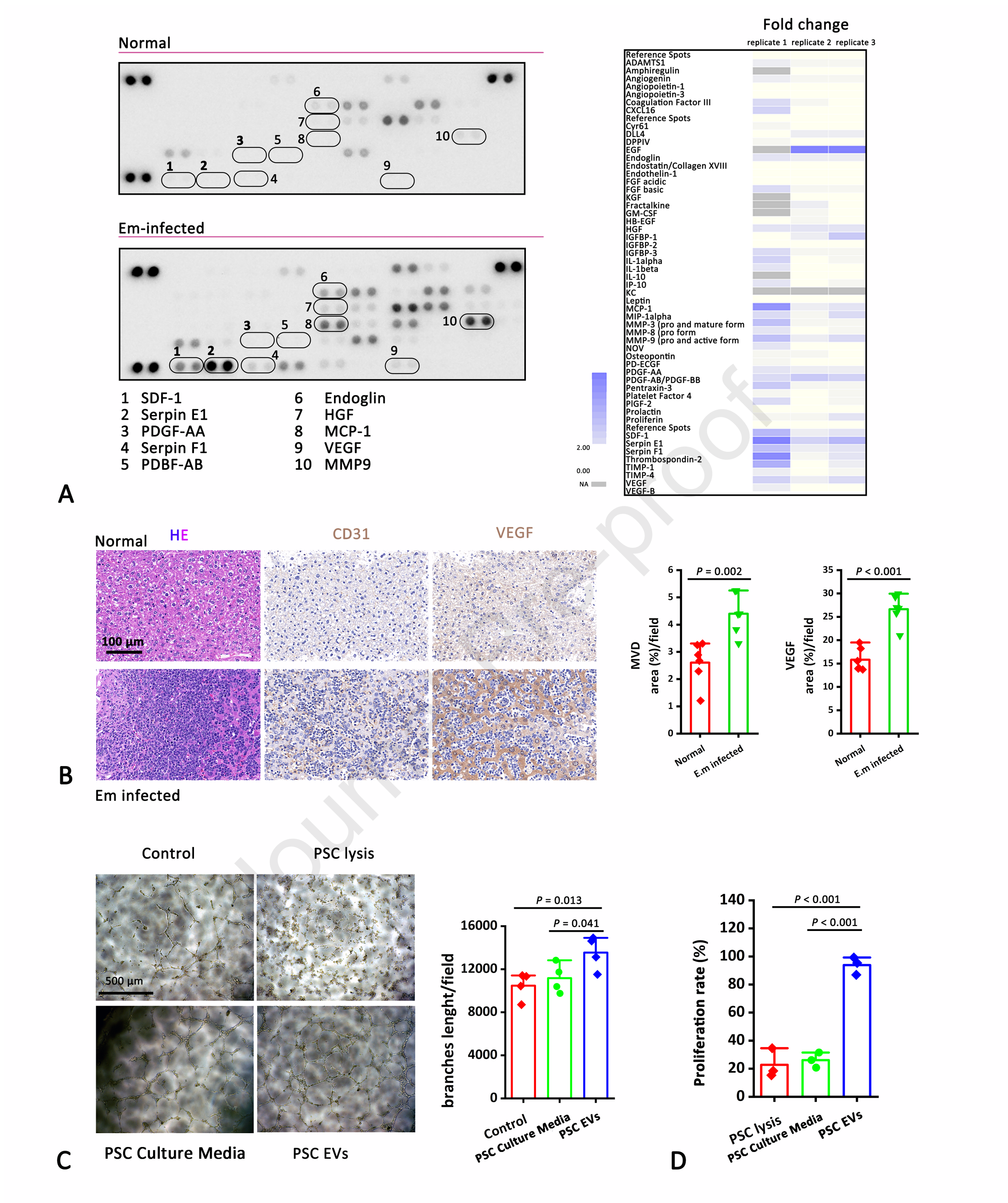
Normal
Em-infected
1 SDF-1
2 Serpin E1
3 PDGF-AA
4 Serpin F1
5 PDBF-AB
6 Endoglin
7 HGF
8 MCP-1
9 VEGF
10 MMP9
A
Fold change
replicate 1
replicate 2
replicate 3
Reference Spots
ADAMTS1
Amphiregulin
Angiogenin
Angiopoietin-1
Angiopoietin-3
Coagulation Factor III
CXCL16
Reference Spots
Cyr61
DLL4
DPPIV
EGF
Endoglin
Endostatin/Collagen XVIII
Endothelin-1
FGF acidic
FGF basic
KGF
Fractalkine
GM-CSF
HB-EGF
HGF
IGFBP-1
IGFBP-2
IGFBP-3
IL-1alpha
IL-1beta
IL-10
IP-10
KC
Leptin
MCP-1
MIP-1alpha
MMP-3 (pro and mature form
MMP-8 (pro form
MMP-9 (pro and active form
NOV
Osteopontin
PD-ECGF
PDGF-AA
PDGF-AB/PDGF-BB
Pentraxin-3
Platelet Factor 4
PlGF-2
Prolactin
Proliferin
Reference Spots
SDF-1
Serpin E1
Serpin F1
Thrombospondin-2
TIMP-1
TIMP-4
VEGF
VEGF-B
2.00
0.00
NA
Normal
HE
CD31
VEGF
100 µm
Em infected
B
MVD area (%)/field
P = 0.002
VEGF area (%)/field
P < 0.001
Normal
E.m infected
Control
PSC lysis
500 µm
PSC Culture Media
PSC EVs
C
branches lenght/field
P = 0.013
P = 0.041
Proliferation rate (%)
P < 0.001
P < 0.001
D

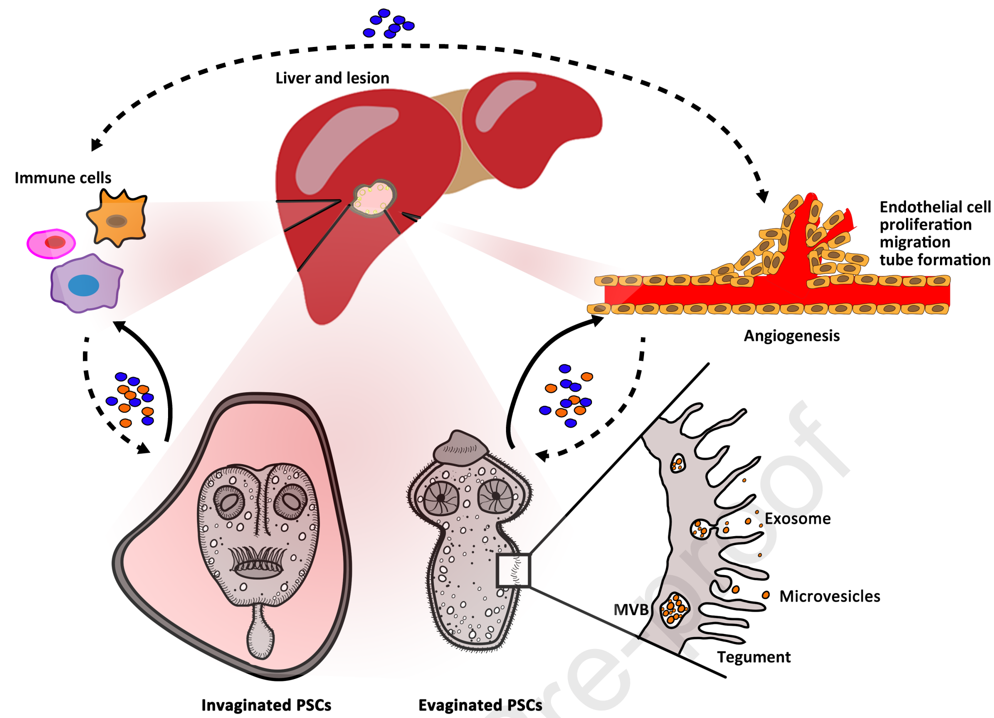
Liver and lesion
Immune cells
Endothelial cell
proliferation
migration
tube formation
Angiogenesis
Exosome
Microvesicles
MVB
Tegument
Invaginated PSCs
Evaginated PSCs